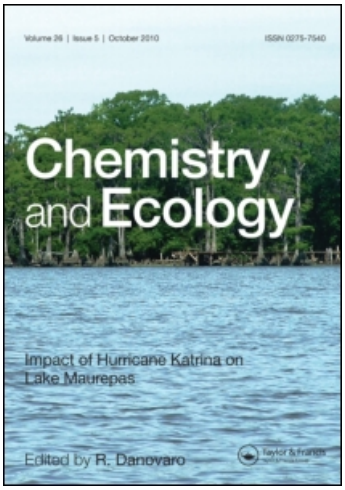

Chemistry and Ecology
Publication details, including instructions for authors and subscription information:
http://www.informaworld.com/smpp/title~content=t713455114

Rare-earth elements and yttrium distributions in mangrove coastal water systems: The western Gulf of Thailand

P. Censi[a]; S. E. Spoto[a]; G. Nardone[b]; F. Saiano[c]; R. Punturo[a]; S. I. Di Geronimo[a]; S. Mazzola[d]; A. Bonanno[d]; B. Patti[d]; M. Sprovieri[e]; D. Ottonello[b]
[a] Department of Geological Sciences, University of Catania, Catania, Italy [b] Department of Botanic Sciences, University of Palermo, Palermo, Italy [c] I.T.A.F., University of Palermo, Palermo, Italy [d] I.A.M.C.-CNR-Sezione di Mazara del Vallo (TP), Mazara del Vallo, Italy [e] I.A.M.C.-CNR-Sezione Geomare, Napoli, Italy

To cite this Article Censi, P. , Spoto, S. E. , Nardone, G. , Saiano, F. , Punturo, R. , Geronimo, S. I. Di , Mazzola, S. , Bonanno, A. , Patti, B. , Sprovieri, M. and Ottonello, D.(2005) 'Rare-earth elements and yttrium distributions in mangrove coastal water systems: The western Gulf of Thailand', Chemistry and Ecology, 21: 4, 255 — 277
To link to this Article: DOI: 10.1080/02757540500213216
URL: http://dx.doi.org/10.1080/02757540500213216

Chemistry and Ecology
Vol. 21, No. 4, August 2005, 255–277

Taylor & Francis
Taylor & Francis Group

Rare-earth elements and yttrium distributions in mangrove coastal water systems: The western Gulf of Thailand

P. CENSI*†, S. E. SPOTO†, G. NARDONE‡, F. SAIANO§, R. PUNTURO†, S. I. DI GERONIMO†, S. MAZZOLA¶, A. BONANNO¶, B. PATTI¶, M. SPROVIERI‖ and D. OTTONELLO‡

†Department of Geological Sciences, University of Catania, Corso Italia, 55 95129 Catania, Italy
‡Department of Botanic Sciences, University of Palermo,Via Archirafi, 32 90123 Palermo, Italy
§I.T.A.F., University of Palermo, Viale delle Scienze, 13 90100 Palermo, Italy
¶I.A.M.C.-CNR-Sezione di Mazara del Vallo (TP) Via L. Vaccara, 61 91026 Mazara del Vallo, Italy
‖I.A.M.C.-CNR-Sezione Geomare, Calata Porta di Massa 80133 Napoli, Italy

(Received 23 February 2005; in final form 24 May 2005)

The concentration of rare-earth elements and yttrium (REY) was investigated in dissolved phase, suspended particulate matter, and seafloor sediments of the western coastal area of the Gulf of Thailand. The samples show Eu and Gd positive anomalies in the shale-normalized REY patterns, especially in the suspended particulate matter. On the other hand, a very high REE content was detected in the coastal waters, probably due to the weathering produced by the Mae Klong river waters on rare-earth element (REE)-rich accessory minerals coming from terrains and mineral deposits cropping out in the studied area. The shale-normalized patterns of yttrium and REE estimated for the dissolved phase show an enrichment of medium rare-earth elements (MREE), characteristic of extensive water–rock interactions and weathering occurring in the continental environment. The REE concentrations of suspended particulate, normalized to the REE concentrations in each sediment sampled from the tidal flat, show the same behaviour of the experimentally determined apparent REE bulk distribution coefficients [1] for pH values ranging from about 5.5 to 6.2. Since the REY concentration of the water masses is controlled by the oceanographic features of the studied area, riverine inputs, and ionic straight, we suppose that the dissolved phase represents a mix of truly dissolved and colloidal pool ($<0.2\,\mu m$) in which REY were enriched during the rock–water interactions of continental environment. In the estuarine system, the salt-induced coagulation of colloidal pool takes place and an authigenic fraction of suspended matter is formed, assuming the typical REE behaviour due to rock–water interactions.

Keywords: Rare-earth elements; Gulf of Thailand; Eu and Gd anomalies

1. Introduction

Geochemical processes in the riverine–marine mixing zone can play an important although currently poorly understood role in the modification of the chemical fluxes of rare-earth elements and yttrium (REY) from continent to seawater.

*Corresponding author. Email: pcensi@unict.it

Chemistry and Ecology
ISSN 0275-7540 print/ISSN 1029-0370 online © 2005 Taylor & Francis
http://www.tandf.co.uk/journals
DOI: 10.1080/02757540500213216

The purpose of this study is to investigate the behaviour of REY in a coastal tropical environment dominated by mangrove forest system. This environment was identified in the Phetchamburi coastal area, in the north-western gulf of Thailand where the effects of large inputs of REY in both dissolved and suspended phases are supplied by the discharge of the Mae Klong river waters that drain highly populated areas and country rocks where REY are concentrated in accessory minerals.

The REY distributions were used in the last three decades as useful tracers of a variety of 'primary' geochemical processes both in igneous petrology and in sedimentology [2]. They have an usual trivalent charge (with the occurrence of Ce^{4+} and Eu^{2+} only under oxiding and reducing conditions, respectively) and show a regular decrease in ionic radius with increase in atomic number. Because of its similar ionic dimensions (intermediate between Dy and Ho) and charge also, Y is generally associated with REE.

On the contrary, in surface environments, this charge- and radius-controlled (CHARAC) REY behaviour [3] is overlapped by a non-CHARAC behaviour that prevails where complexation in the seawater and competitive scavenging processes onto surfaces of suspended particulate matter in water masses take place. REY that are particle-reactive can form strong dissolved complexes with inorganic and organic ligands (carbonate and phosphate ions and ethylendiaminetetraacetic acid) [4–9] and can adsorb onto the surface coating of Mn and Fe oxydroxides. These processes are controlled by the electronic configurations of the involved ions, causing different chemical behaviour for Y and REE and light REE (from La to Eu) and heavy REE (from Gd to Lu). These phenomena allowed many researchers to employ REY as tracers of environmental characters, allowing a clear discrimination between aquatic environments characterized by different ionic strength conditions [10]. This approach results in an ideal geochemical tool to investigate the chemical land–sea system, especially in coastal areas where large mangrove forests occur.

The dissolved concentrations of REY in riverine–coastal seawater areas were extensively studied in order to define the chemical behaviour of the REY in continental and marine environments [11–14]. During these studies, small but nevertheless significant differences among REE distributions were observed and justified by the so-called 'lanthanide contraction effect' typical of various geochemical processes influencing the lithospheric and marine environments. Under these conditions, large-scale removal of dissolved REY that reduces the fluxes of these elements from the continent to the ocean and affects the budget of these elements was observed and explained by various factors such as: (1) carbonate uptake, (2) coprecipitations with hydroxydes [1] and (3) coagulation of the colloidal phase in a hyposaline interface zone [14–15]. On the other hand, REE complexation in natural waters demonstrated the importance of carbonate ion complexes in neutral or high-pH waters [16–19] and in the free metal REE^{3+} and REE–sulphate complexes in acidic intermediate and saline environments [19].

Ultimately, the Kingdom of Thailand is one of the most important REE world producers, but very limited investigations have been carried out in coastal waters of Thailand to evaluate the REY distributions.

The investigations carried out during this research provide a detailed dataset of REY concentrations in coastal waters, particulate, and marine sediments collected in the upper part of the tidal flat zone of the Phetchamburi coastal area. The geographical distribution of the studied stations offers the opportunity to evaluate the REY distribution in an area where the composition of seawater in terms of REE contents has not been extensively monitored, and the effects of large inputs of REY in a typical mangrove environment are not well known. Moreover, this study allows us to recognize and distinguish the REE input of natural origin due to weathering of country rocks from other enthropogenic sources.

2. Material and methods

2.1 *Study area*

The area under investigation is highly populated and is characterized by the presence of mineral deposits located in the Meklong Highlands, a remote jungle region in the Kanchanaburi Province. Here, near the Burma border, is the Western Granitoid Province of Thailand. This represents one of the most important areas for tin production in Southeast Asia [20]. These terrains are almost exclusively made up of biotite-bearing granites and granodiorites of Cretaceous to Tertiary age. Moreover, the weathering of these primary deposits gave way from the formation of secondary tin deposits in which REE-rich minerals such as xenothime and monazite, owing to their chemical resistance and stability, are associated with tin-bearing minerals, mainly cassiterite, to form secondary alluvial placers.

The occurrence of present-day and historic mining activities produces high concentrations of heavy metals transported by the fluvial system. This process is controlled by mineralogical features and the behaviour of metal-bearing mineral particles. No data are available in the scientific literature regarding the REY loads both transported by the fluvial systems and present in the coastal water system of the investigated region. On the other hand, knowledge of these parameters has strong relevance due to the highly populated region, the rapid increase in population in this area, and the industrialization and economic development occurring there [21]. Moreover, the coastal area studied here is a good example of mangrove environment and related closed environmental conditions with a high O_2 consumption induced by the oxidation of organic matter in turn producing large changes in redox and pH conditions [21] that influence the partition coefficients of trace elements among dissolved, suspended, and sedimentary phases. The two largest rivers of Thailand, Chao Phraya and Mae Klong, are present in the study area with an annual water discharge of 13 km^3, corresponding to a mean flux of 412 100 $m^3\ s^{-1}$, and an annual suspended sediment discharge of 8.1 million tonnes [22]. The seasonal water discharge reaches a maximum during the period between August and November, while during February to May, water discharge falls to about 100 $m^3\ s^{-1}$ [23].

2.2 *Sampling strategies and analytical methods*

Sampling strategies are reported in [24] and location of investigated sampling stations are reported in figure 1.

2.2.1 Sampling of seawater, suspended particulate and sediments. Water samples were collected from a fishing boat using a hand-made polyethylene sampler consisting of a 5 l Niskin bottle. Upon recovery of the bottles, water samples were filtered through 0.2 μm Millipore® filters, using a Teflon tubing apparatus. The filtration was done immediately on board, and samples were always transported within 8 h to the laboratory. Filtered samples were acidified to pH 1–2 with HNO_3 (Merck ULTRAPUR®) and stored in hot-acid-washed polyethylene bottles.

Seafloor sediments were sampled with a Van Veen bucket in the same stations where seawater and suspended materials in the water column were collected.

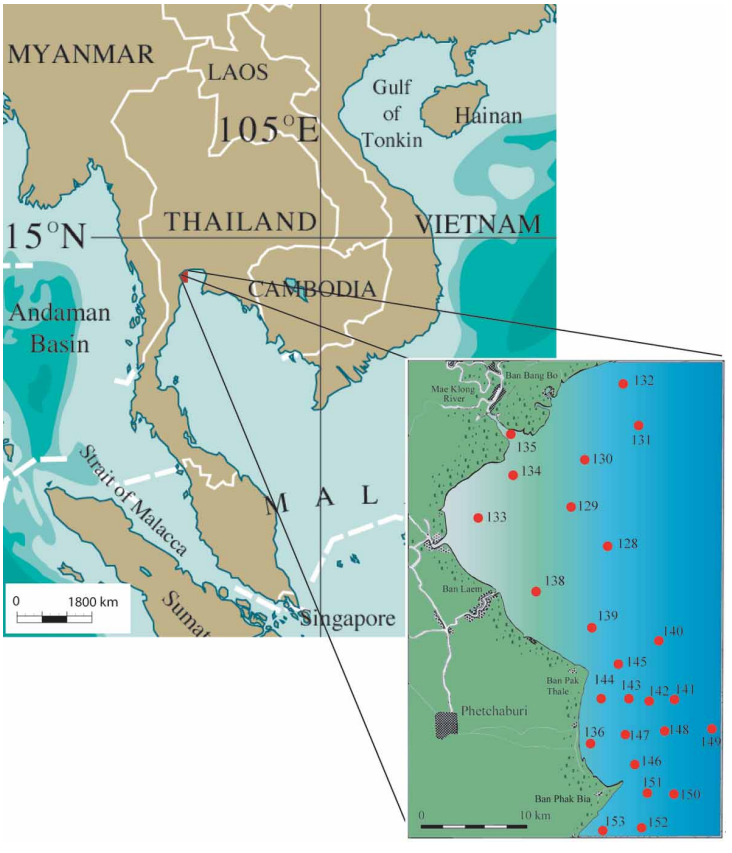

Figure 1. Location map of the study area. Sampling sites are also reported.

In order to increase the signal/noise ratio in the studied seawaters, for Y and REE analyses 1000 ml of each sample was pre-concentrated with a CHELEX 100® (100–200 mesh) ion-exchange resin:

- pH value of each seawater sample was set to 6.0 ± 0.1 with CH_3COONH_4, and an aliquot of each seawater sample passed on an 8-cm-long column filled with CHELEX-100 100–200 mesh previously cleaned and conditioned [25].
- REY were eluted with 5 ml of HNO_3 3.5 M, giving a 100-fold enrichment factor. Details of the procedures are reported in the literature [25, 26].
- Seafloor sediments were sampled with a VanVeen bucket at the same stations where seawater and suspended materials in the water column were collected.

2.2.2 Analytical methodologies. To evaluate the REY recovery and accuracy of the pre-concentration method used for the study samples, 10 l of an artificial seawater standard solution were prepared according to the procedure described below:

- 10 l of seawater was filtered and treated as a normal sample.
- Samples were pre-concentrated by means of an 8-cm-long column filled with CHELEX-100, 100–200 mesh, as reported above. All the dissolved trace elements were then removed

onto CHELEX resin. This procedure was repeated five times to remove all the trace element originally contained in seawater. This solution was named SOL-1.

- Then, 500 µl of a standard solution containing 10 ppb of all the REE and Y were added to SOL-1 to obtain 5 l of a solution containing 10 ppt of dissolved REY in the seawater matrix given by SOL-1. This solution was named AAPS (see table 1).
- Five different recovery procedures were carried out using AAPS, using 1 l of AAPS that was pre-concentrated with CHELEX 100® for five different times (EL-1, 2, 3, 4, 5).
- The amount of recovery for REY for each experiment was calculated and reported in table 1 (EL-1, EL-2, EL-3, EL-4, EL-5).
- The eluted fractions for samples and standard solutions were analysed with a high resolution ICP-MS (ThermoFinniganMAT Element 2) using 100 ppt Rh as an internal standard. The measurements were carried out in high-resolution mode allowing the signal of the elements to be separated from those of most isobaric interferences as BaO^+.

Analytical blanks were obtained with 50 ml of HNO_3 Merck Ultrapure in Millipore ultrapure water (18.2 MΩ/cm), and concentrations were negligible compared with measured REE concentrations. Five aliquots of these ultrapure solutions were analysed five times, and the standard deviations calculated from the average values measured (table 1). The detection limits were evaluated as three times the standard deviations measured for analytical blanks [27] and are listed in table 1.

In order to evaluate the contribution of REE and Y released from CHELEX-100 and chemicals used during concentration procedures, a set of five procedural blanks was prepared using Millipore ultra-pure water with the same quantities of all chemicals used to concentrate the investigated trace elements from seawater. The results indicate that the amounts of trace metals lost during recovery procedures and sampling manipulations are negligible with respect to the mean values of dissolved fraction recorded in the seawater samples (see PB-1, 2, 3, 4, 5 in Table 1).

Particulate fractions, on the filters were digested using a microwave oven CEM Mars 5 according to procedures reported in the literature [24]. The solutions from both particulate and sedimentary samples were directly analysed after a 1:50 dilution with 5% HNO_3 Merck ULTRAPUR® solution adding 100 ppt Rh solution as an internal standard.

All the analysed solutions were treated under a laminar air flow clean bench to minimize contamination risks and were prepared with high-purity-grade reagents (Merck Ultrapure®).

2.2.3 GIS treatment and statistical evaluation of chemical data. Area mapping of the heavy metal contents followed a specific procedure carried out using the program WGeo (Wasi Gmbh). 2D zone maps were drawn using the GIS program ArcView 8.3 (Environmental Systems Research Institute, Inc.), upgraded with the '3D ANALYST' extension, which allowed the discrete data to be transformed into a continuous distributional model. In order to evaluate a mathematical operator to interpolate area chemical data, an exact interpolator (IDW Inverse Distance Weighting) was used. Thus, all data reported in the showed maps are exact values in the sampling points and interpolated values among them.

3. Results

3.1 *Dissolved phases*

The REY of the dissolved phase are reported in table 2, while in figure 2, dissolved surface REY distributions in the studied area are shown. The values are often higher than those reported

Table 1. Measured mass, average of five different determinations of analytical blank concentrations (Bl. conc.), related standard deviations, detection limits of analyses, elemental concentrations both in procedural blanks (PB-1, PB-2, PB-3, PB-4, PB-5), in artificially prepared seawater standard (APSS) and eluted fractions (EL-1, EL-2, EL-3, EL-4, EL-5) and related recovery values measured*.

Analytical blank			Procedural blank							Standard concentration						Recovery %						
Bl. conc.	$\pm\sigma$	D.L.	PB-1	PB-2	PB-3	PB-4	PB-5	Mean	$\pm\sigma$	APSS	EL-1	EL-2	EL-3	EL-4	EL-5	EL-1	El-2	EL-3	EL-4	EL-5	Mean	$\pm\sigma$
0.83	0.12	0.36	0.91	0.96	1.10	1.07	1.11	1.03	0.09	112.47	101.81	105.72	104.55	105.67	102.53	90.52	94.00	92.96	93.95	91.16	92.52	1.60
0.35	0.18	0.53	0.42	0.91	0.92	0.99	1.03	0.86	0.25	71.99	68.49	66.52	69.18	66.43	66.86	95.14	92.40	96.09	92.28	92.87	93.75	1.74
0.08	0.01	0.04	0.21	1.01	1.16	1.13	1.16	0.94	0.41	71.37	69.41	66.94	72.18	65.81	68.91	97.25	93.80	101.14	92.21	96.56	96.19	3.44
0.20	0.06	0.18	0.17	1.18	0.91	0.93	0.91	0.82	0.38	70.97	64.35	65.49	62.45	64.21	64.14	90.67	92.28	87.99	90.47	90.38	90.36	1.53
0.09	0.05	0.15	0.16	1.15	1.09	0.94	1.07	0.88	0.41	69.33	64.02	65.82	63.46	66.33	66.81	92.34	94.94	91.54	95.67	96.37	94.17	2.12
0.05	0.02	0.05	0.08	1.11	1.02	1.16	1.11	0.90	0.46	66.51	64.36	65.44	64.88	61.41	61.79	96.78	98.39	97.56	92.33	92.91	95.59	2.78
0.31	0.15	0.46	0.07	1.06	0.98	1.05	0.91	0.81	0.42	65.81	59.34	61.45	61.09	57.65	59.96	90.18	93.38	92.83	87.60	91.11	91.02	2.30
0.22	0.13	0.40	0.09	1.13	1.11	1.11	0.90	0.87	0.45	63.59	58.39	56.71	57.28	55.35	58.18	91.82	89.18	90.07	87.04	91.48	89.92	1.93
0.30	0.05	0.14	0.11	1.05	1.10	0.97	0.98	0.84	0.41	62.92	58.56	60.68	59.11	57.41	60.87	93.06	96.44	93.93	91.24	96.74	94.28	2.32
0.48	0.19	0.56	0.08	0.96	1.08	1.06	1.14	0.86	0.44	61.54	57.81	59.46	54.70	58.01	59.60	93.95	96.63	88.89	94.27	96.85	94.12	3.21
0.07	0.04	0.12	0.06	0.91	1.16	1.00	0.96	0.82	0.43	60.63	56.67	54.33	57.84	53.69	54.27	93.46	89.61	95.40	88.56	89.51	91.31	2.96
0.02	0.01	0.02	0.05	1.03	0.96	0.97	1.14	0.83	0.44	59.79	54.64	51.95	54.17	54.30	49.15	91.40	86.90	90.60	90.82	82.21	88.38	3.88
0.03	0.01	0.02	0.04	0.96	0.99	0.92	1.06	0.79	0.42	59.20	54.64	56.35	55.95	53.42	57.07	92.30	95.19	94.52	90.25	96.40	93.73	2.45
0.02	0.01	0.02	0.07	1.04	1.17	0.94	1.00	0.84	0.44	57.79	53.87	56.94	57.02	54.98	52.84	93.22	98.53	98.67	95.14	91.43	95.40	3.20
0.02	0.01	0.02	0.06	1.05	1.09	1.06	1.12	0.88	0.46	57.15	53.99	53.64	51.36	51.02	54.50	94.47	93.85	89.87	89.28	95.36	92.57	2.79

*All the concentration values are given in pmol l^{-1}. For detailed explanations, see text.

Table 2. Station numbers, sampling depth, geographic location, and REY concentrations in the dissolved fraction of seawater samples.

Station no.	Sampling depth (m)	Latitude (North)	Longitude (East)	Y nmol l^{-1}	La nmol l^{-1}	Ce nmol l^{-1}	Pr pmol l^{-1}	Nd nmol l^{-1}	Sm pmol l^{-1}	Eu pmol l^{-1}	Gd pmol l^{-1}	Tb pmol l^{-1}	Dy pmol l^{-1}	Ho pmol l^{-1}	Er pmol l^{-1}	Tm pmol l^{-1}	Yb pmol l^{-1}	Lu pmol l^{-1}
128a	0.5	13° 15.883′	100° 04.457′	1.38	0.89	2.04	249.45	0.90	188.55	33.89	182.19	21.08	117.85	22.13	62.78	7.10	41.32	8.86
129a	0.5	13° 17.931′	100° 05.451′	0.55	0.28	0.35	48.61	0.17	33.59	7.90	33.07	5.98	31.08	7.28	21.22	2.96	21.78	3.71
130a	0.5	13° 20.450′	100° 04.212′	3.34	2.33	5.37	634.09	2.20	470.87	91.80	414.94	64.81	299.38	54.87	159.93	18.35	142.74	17.72
131a	0.5	13° 21.228′	100° 06.419′	0.57	0.26	0.33	45.61	0.20	31.59	6.91	38.47	6.29	32.92	9.52	34.00	7.40	57.82	10.32
132a	0.5	13° 24.100′	100° 06.400′	2.55	1.69	4.06	476.90	1.66	343.18	60.54	313.51	46.88	216.00	38.50	114.49	20.42	162.97	27.77
133a	0.5	13° 18.555′	100° 01.997′	3.04	2.05	4.90	551.42	1.92	402.37	72.72	360.89	53.80	264.62	46.38	136.91	17.17	108.65	14.86
134a	0.5	13° 17.906′	100° 00.850′	3.18	2.38	5.69	655.38	2.26	464.22	82.26	402.23	62.61	304.92	54.87	153.35	18.35	102.87	14.86
135a	0.5	13° 21.720′	99° 59.978′	1.49	1.25	2.70	314.03	1.08	213.82	41.46	205.41	28.95	142.15	25.47	66.36	8.29	46.81	7.14
138a	0.5	13° 10.166′	100° 05.036′	3.72	2.60	6.39	769.64	2.79	595.57	100.36	514.47	77.71	369.23	66.09	191.32	20.13	123.38	16.00
140a	0.5	13° 10.359′	100° 05.745′	0.32	0.42	0.20	29.58	0.11	19.62	5.59	27.91	5.04	31.00	7.51	22.46	4.14	29.72	4.86
141a	0.5	13° 10.250′	100° 07.945′	0.36	0.22	0.30	38.68	0.12	24.94	4.28	26.71	4.09	25.67	4.85	14.65	2.37	17.79	3.14
142a	0.5	13° 07.945′	100° 08.229′	0.47	0.18	0.37	46.48	0.15	34.92	9.87	35.61	7.24	31.69	8.49	25.73	3.85	28.32	4.86
143a	0.5	13° 08.141′	100° 07.332′	0.96	0.65	1.48	168.90	0.59	122.04	24.35	112.56	15.73	86.15	15.46	43.94	5.33	28.61	4.57
144a	0.5	13° 08.068′	100° 06.537′	4.97	4.00	9.91	1053.15	3.64	767.82	155.30	748.81	110.12	557.54	99.13	272.93	30.19	184.35	23.43
145a	0.5	13° 07.883′	100° 05.989′	0.96	0.72	1.59	184.16	0.62	127.36	25.99	120.51	16.99	92.00	16.37	46.04	5.03	31.50	4.29
146a	0.5	13° 08.905′	100° 06.102′	1.77	1.25	2.90	350.58	1.22	250.07	48.70	231.48	33.98	171.08	28.19	83.10	9.47	54.61	8.00
147a	0.5	13° 06.586′	100° 06.303′	0.38	0.15	0.24	31.23	0.10	22.28	4.61	23.38	4.09	27.13	5.15	13.75	2.37	17.10	2.29
148a	0.5	13° 06.480′	100° 07.861′	0.43	0.17	0.29	35.13	0.13	25.61	6.25	25.76	3.78	26.15	6.06	18.83	2.37	17.54	2.86
149a	0.5	13° 06.432′	100° 08.499′	0.20	0.07	0.09	13.13	0.06	10.64	2.63	11.06	1.89	12.00	3.33	10.34	1.52	12.62	2.47
150a	0.5	13° 06.399′	100° 09.585′	0.37	0.61	0.25	30.16	0.14	24.94	5.59	26.96	4.40	24.92	5.76	17.94	2.66	22.24	2.86
151a	0.5	13° 02.753′	100° 08.132′	0.56	0.40	0.93	98.64	0.34	72.49	20.73	75.68	12.90	56.92	11.82	31.69	5.03	37.68	6.29
152a	0.5	13° 02.779′	100° 07.041′	0.30	0.14	0.24	32.64	0.13	24.61	8.23	33.02	7.51	41.72	9.44	30.23	4.74	35.41	6.29
153a	0.5	13° 01.046′	100° 06.946′	0.44	0.31	0.64	74.52	0.25	52.87	11.85	56.28	8.81	39.08	7.88	20.33	2.66	15.74	2.29

(*continued*)

Table 2. Continued

Station no.	Sampling depth (m)	Latitude (North)	Longitude (East)	Y nmol l^{-1}	La nmol l^{-1}	Ce nmol l^{-1}	Pr pmol l^{-1}	Nd nmol l^{-1}	Sm pmol l^{-1}	Eu pmol l^{-1}	Gd pmol l^{-1}	Tb pmol l^{-1}	Dy pmol l^{-1}	Ho pmol l^{-1}	Er pmol l^{-1}	Tm pmol l^{-1}	Yb pmol l^{-1}	Lu pmol l^{-1}
128b	5.0	13° 10.250′	100° 07.945′	0.52	0.27	0.33	48.26	0.15	33.92	8.23	33.39	6.92	31.69	6.97	23.91	3.26	25.12	4.57
129b	5.0	13° 07.945′	100° 08.229′	0.42	0.22	0.27	39.03	0.12	23.94	5.92	26.07	4.09	26.15	4.85	15.25	2.07	17.10	3.05
140b	7.0	13° 06.480′	100° 07.861′	0.31	0.14	0.18	25.55	0.08	18.29	3.95	18.76	3.32	19.38	3.94	11.96	2.07	14.73	2.00
141b	8.0	13° 06.432′	100° 08.499′	0.34	0.16	0.27	35.48	0.11	24.28	5.92	23.85	3.78	23.04	4.85	14.05	2.37	17.30	2.29
147b	7.0	13° 02.753′	100° 08.132′	0.82	0.60	1.32	145.84	0.52	107.41	22.37	103.34	14.47	83.69	15.76	42.45	4.44	27.16	4.00
148b	8.0	13° 15.883′	100° 04.457′	0.47	0.23	0.43	52.16	0.18	40.24	9.54	34.66	6.29	40.00	7.28	22.72	3.25	20.66	2.86
150b	8.0	13° 17.931′	100° 05.451′	0.57	0.31	0.68	79.48	0.26	58.53	17.11	53.10	10.38	44.31	12.43	26.01	5.92	45.20	7.44
128c	9.0	13° 20.450′	100° 04.212′	0.38	0.14	0.17	31.23	0.12	20.28	3.95	23.85	4.09	24.18	4.55	16.44	2.37	20.52	3.71
129c	9.0	13° 21.228′	100° 06.419′	0.91	0.55	1.25	149.39	0.51	104.42	22.70	98.57	15.10	70.15	14.85	40.36	6.22	43.36	6.29
130c	5.0	13° 10.250′	100° 07.945′	0.79	0.48	0.88	107.87	0.35	75.49	16.12	77.58	12.27	56.92	11.82	34.68	5.62	45.20	7.90
131c	5.0	13° 07.945′	100° 08.229′	0.75	0.47	1.02	131.64	0.42	92.11	21.72	90.94	14.16	63.69	13.04	37.37	5.89	51.06	9.72
140c	15.0	13° 08.141′	100° 07.332′	0.73	0.39	0.75	95.81	0.31	68.17	11.85	64.55	10.38	49.85	11.22	32.58	4.61	26.01	4.57
141c	16.0	13° 06.432′	100° 08.499′	0.47	1.82	1.89	266.13	0.27	45.56	12.17	86.80	8.18	37.85	8.49	23.91	4.44	15.60	4.57
142c	11.0	13° 06.399′	100° 09.585′	1.03	0.71	1.65	179.90	0.61	126.36	25.34	117.97	16.99	91.08	17.89	46.93	5.33	28.90	4.29
148c	17.0	13° 02.753′	100° 08.132′	0.52	0.29	0.68	79.48	0.28	56.86	11.52	51.51	8.31	42.46	8.19	23.32	2.96	20.38	2.86
149c	18.0	13° 02.779′	100° 07.041′	0.44	0.29	0.54	66.71	0.22	49.88	13.49	47.06	9.12	40.62	10.61	32.17	4.74	36.91	5.14
150c	16.0	13° 01.046′	100° 06.946′	0.42	0.31	0.65	72.74	0.24	53.21	12.50	47.38	8.81	37.85	8.49	21.82	3.55	25.59	4.58
151c	7.5	13° 15.883′	100° 04.457′	0.93	1.32	1.70	189.13	0.65	136.67	25.66	131.96	19.19	100.62	18.49	46.63	5.92	32.36	4.57
152c	12.0	13° 17.931′	100° 05.451′	0.55	0.37	0.79	95.81	0.33	68.17	11.85	65.82	9.75	50.15	8.79	26.31	3.26	20.80	2.86

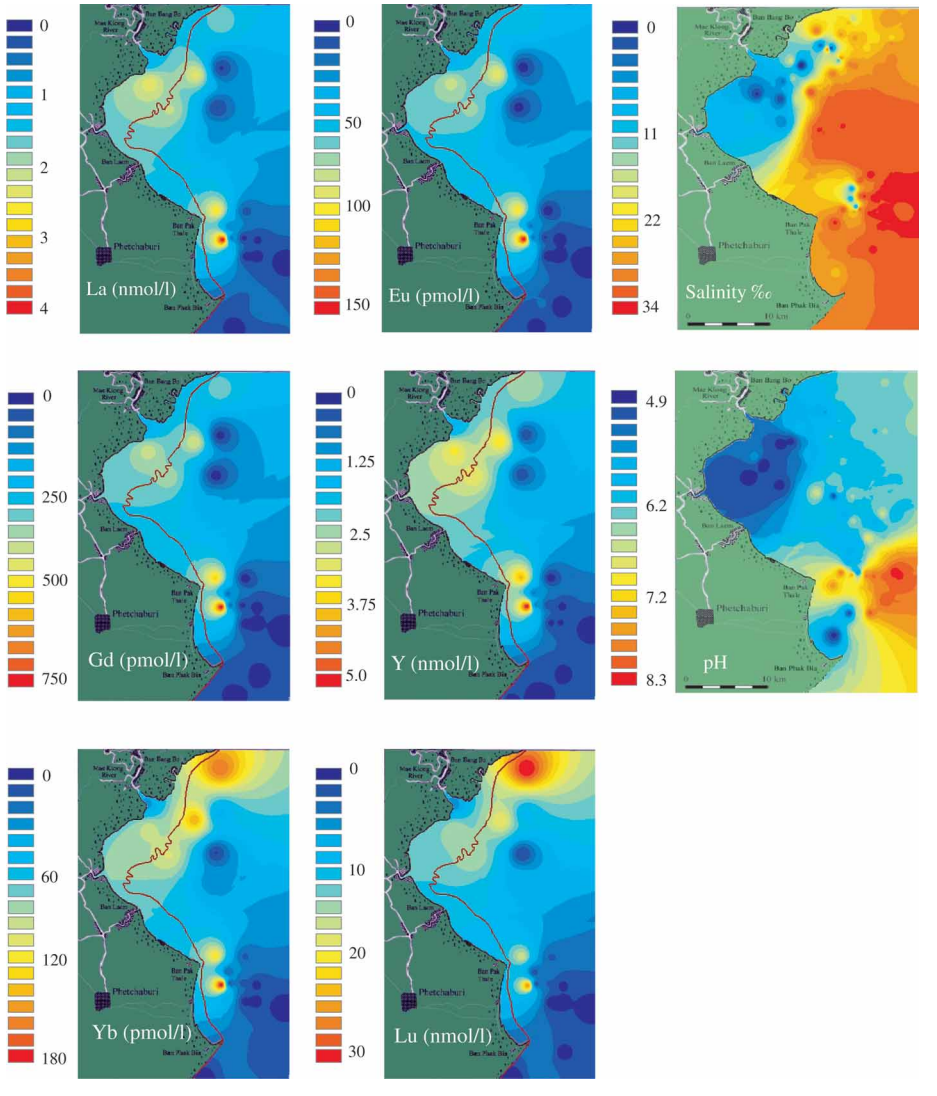

Figure 2. Schematic distribution of selected rare earth elements and Y in the dissolved fraction of surface water samples. For further details on the statistical treatment of chemical data, see text. The distributions of salinity and pH values are given for reference. The original data of pH and salinity are reported in the literature [33]. Red lines indicate the seaward limit of the tidal flat.

for typical coastal marine environments characterized by riverine inputs. They reach values of up to about 4 nmol l^{-1} for La and about 10 nmol l^{-1} for Ce contents in station 144, although generally all the studied trace elements show homogeneous distribution.

A homogeneous trend toward the increase in REE contents in dissolved phase is observed in the south-eastern area according with increasing depth, while only the Y and heavy REE are enriched in the Mae Klong estuary system, along the north-eastern coast. For these elements, concentration values decrease to normal marine values in a southeasterly direction with increasing salinity and pH values [28].

3.2 *Particulate matter*

The REY contents in the particulate fraction are reported in table 3. The concentration values measured for suspended particulate matter confirm that in this fraction, large amounts of lithogenic materials, coming from weathering and erosion of country rocks, occur.

The distribution of suspended particulate matter in surface waters (figure 3) shows that the highest REE concentrations are reported in the northern studied area, especially in the Mae Klong estuarine zone. Only the Y distribution is different, showing a minimum concentration in suspended particulate matter from the Mae Klong estuary and larger concentrations in southern and eastern sampling areas toward the Chao Phraya river estuary.

3.3 *Sediments*

The distribution of REE values in seafloor sediments is reported in table 4. This shows that a large enrichment in REY content in sediments occurs in the north-eastern area where large inputs from the Chao Phraya and Mae Klong river estuaries are located (figure 4). A decrease in REE content is observed in a south-eastward direction. Only the La distribution shows a different behaviour with a maximum in the southern part of the sampled area.

3.4 *Shale-normalized and chondrite-normalized REY patterns*

The concentrations of REE and Y in seawater are generally normalized to shale composition in order to identify the sources of REE and Y in seawater (weathering of outcropping rocks in the surrounding areas of the basin, atmospheric input by dry or wet deposition, etc.) and the mechanisms of transport of the trace elements to the oceans (rivers, estuaries, etc.). In fact, the REY signature of sediments and waters originates on a mix of continental crust sources that usually show a typical shale signature [29–30], and then the shale-normalized REY pattern of seawaters is normally considered a useful tool to emphasize the behaviour of REY in the marine system.

The surface and intermediate waters REY distribution patterns normalized to PAAS (Post Archean Australian Shales) [29] show that less concentrated water samples (sample/PAAS values less than 1 for La) have REY distributions similar to those reported for Japanese rivers [31] with HREE enrichment related to LREE, typical for coastal marine waters (figure 5). In contrast, shale-normalized REY distributions with high REY concentrations (sample/PAAS values greater than 1 for La) show a flat behaviour with a limited intermediate MREE enrichment centred on Eu and Gd.

At the same time, shale-normalized REY patterns in suspended particulate (figure 6) collected in surface waters show a behaviour characterized by:

- a small La negative anomaly;
- a flat behaviour with a little fractionation of LREE/HREE and/or a weak HREE enrichment;
- large Eu and Gd positive anomalies.

In order to evaluate the effects of weathering and transport of continental materials on the REY distribution patterns calculated for the seafloor sediments, a normalization to chondrite composition was carried out [32]. The obtained REY patterns (figure 7) show a LREE/HREE fractionation and an Eu negative anomaly [33].

Table 3. Station numbers, sampling depth, and REY concentrations (mg kg^{-1}) in suspended particulate fractions from seawater samples.

Station no.	Sampling depth (m)	Latitude (North)	Longitude (East)	Y mg kg^{-1}	La mg kg^{-1}	Ce mg kg^{-1}	Pr mg kg^{-1}	Nd mg kg^{-1}	Sm mg kg^{-1}	Eu mg kg^{-1}	Gd mg kg^{-1}	Tb mg kg^{-1}	Dy mg kg^{-1}	Ho mg kg^{-1}	Er mg kg^{-1}	Tm mg kg^{-1}	Yb mg kg^{-1}	Lu mg kg^{-1}
128a	0.5	13° 15.883′	100° 04.457′	11.334	2.389	17.227	2.884	9.454	2.015	5.399	58.823	0.952	2.632	0.492	1.333	0.167	1.315	0.347
128b	0.5	13° 15.883′	100° 04.457′	14.676	5.163	24.248	3.930	14.316	1.338	7.591	64.453	0.249	2.540	0.642	1.682	0.132	2.139	0.600
128c	0.5	13° 15.883′	100° 04.457′	25.970	14.154	54.344	8.665	34.749	6.575	11.264	168.249	1.778	6.945	1.694	4.418	0.725	5.691	1.348
129a	0.5	13° 17.931′	100° 05.451′	12.987	3.570	12.548	3.216	11.378	2.423	5.377	31.477	0.868	2.135	0.479	1.477	0.230	2.225	0.549
129b	0.5	13° 17.931′	100° 05.451′	24.312	1.636	45.518	7.373	27.593	4.133	1.686	176.317	0.780	5.779	1.454	3.616	0.537	5.122	1.332
129c	0.5	13° 17.931′	100° 05.451′	21.838	1.245	41.655	6.369	24.215	3.664	1.472	113.695	0.640	4.675	1.845	3.945	0.400	3.852	0.899
130a	0.5	13° 20.450′	100° 04.212′	15.972	6.432	25.172	4.949	14.500	3.325	8.672	149.992	0.695	4.734	1.158	2.772	0.436	4.169	1.632
130c	0.5	13° 20.450′	100° 04.212′	13.369	8.215	37.219	6.579	23.372	3.629	4.433	77.172	0.445	3.294	0.848	2.196	0.377	2.952	0.900
131a	0.5	13° 21.228′	100° 06.419′	21.153	9.283	37.685	5.477	16.800	3.113	12.656	57.285	0.527	3.884	0.897	2.582	0.318	3.398	0.876
131c	0.5	13° 21.228′	100° 06.419′	24.228	2.549	58.632	9.262	34.524	4.878	1.846	12.923	0.812	5.646	1.342	3.615	0.495	4.626	1.137
132a	0.5	13° 24.100′	100° 06.400′	14.368	12.516	44.159	6.795	25.318	3.844	2.971	2.785	0.545	3.928	0.885	2.712	0.376	2.963	0.596
133a	0.5	13° 18.555′	100° 01.997′	23.455	19.843	66.113	9.430	35.532	6.226	12.811	47.617	0.889	5.612	1.214	3.738	0.572	5.172	1.218
134a	0.5	13° 17.906′	100° 00.850′	21.288	24.182	84.597	12.917	48.598	8.119	4.260	21.557	1.565	6.966	1.547	4.787	0.713	5.213	0.984
135a	0.5	13° 05.493′	100° 04.428′	4.982	38.549	139.977	22.259	82.374	14.239	14.368	265.277	1.982	13.117	3.474	8.292	1.338	10.721	2.412
136a	0.5	13° 10.166′	100° 05.036′	13.174	21.686	82.664	12.922	58.911	9.882	2.236	22.943	0.984	5.577	1.158	3.487	0.564	3.753	0.699
138a	0.5	13° 10.359′	100° 05.745′	17.329	15.632	56.858	8.887	33.712	5.855	3.655	51.124	0.893	6.163	1.385	4.339	0.786	5.213	1.869
139c	0.5	13° 10.250′	100° 07.945′	13.264	14.494	54.196	8.658	33.419	5.986	4.277	5.137	0.759	4.450	1.184	2.915	0.466	3.744	0.851
140a	0.5	13° 07.945′	100° 08.229′	18.353	6.398	25.758	4.894	18.264	2.269	8.642	79.472	0.429	3.717	0.965	2.420	0.257	3.259	0.876
140b	0.5	13° 08.141′	100° 07.332′	3.315	12.763	5.494	8.165	31.236	4.825	15.238	26.966	0.857	6.358	1.614	4.981	0.555	5.268	1.331
141a	0.5	13° 08.141′	100° 07.332′	1.586	1.825	14.551	2.667	8.174	2.537	4.297	58.746	0.813	2.632	0.446	1.496	0.319	1.462	0.433
141b	0.5	13° 08.068′	100° 06.537′	25.936	21.915	62.615	9.893	36.875	5.147	11.554	128.571	0.868	6.369	1.435	3.862	0.529	4.946	1.216
141c	0.5	13° 08.068′	100° 06.537′	1.764	7.417	33.538	5.463	2.772	2.985	4.197	56.692	0.359	2.464	0.612	1.655	0.200	2.861	0.562

(*continued*)

Table 3. Continued

Station no.	Sampling depth (m)	Latitude (North)	Longitude (East)	Y mg kg^{-1}	La mg kg^{-1}	Ce mg kg^{-1}	Pr mg kg^{-1}	Nd mg kg^{-1}	Sm mg kg^{-1}	Eu mg kg^{-1}	Gd mg kg^{-1}	Tb mg kg^{-1}	Dy mg kg^{-1}	Ho mg kg^{-1}	Er mg kg^{-1}	Tm mg kg^{-1}	Yb mg kg^{-1}	Lu mg kg^{-1}
142a	0.5	13° 08.068′	100° 06.537′	17.417	6.758	29.359	4.792	17.235	2.638	6.166	72.942	0.362	3.143	0.819	2.881	0.224	2.623	1.192
142c	0.5	13° 07.883′	100° 05.989′	23.413	14.313	54.557	8.727	32.847	5.252	1.632	114.628	0.838	5.736	1.439	3.848	0.572	4.947	1.187
143a	5.0	13° 07.883′	100° 05.989′	15.642	7.558	31.783	4.794	17.789	2.532	6.933	36.324	0.433	3.128	0.739	2.230	0.269	3.294	0.759
144a	5.0	13° 08.905′	100° 06.102′	15.116	8.955	74.526	11.548	44.635	7.823	2.893	28.295	0.913	5.738	1.291	3.945	0.619	4.236	0.823
145a	7.0	13° 06.586′	100° 06.303′	27.882	17.626	62.723	8.629	39.227	7.577	12.287	27.127	1.127	7.528	1.747	5.211	0.842	6.481	1.593
146a	8.0	13° 06.480′	100° 07.861′	15.626	9.535	31.474	5.837	19.425	2.611	5.937	86.543	0.461	3.514	0.864	2.246	0.294	2.998	0.764
147a	7.0	13° 06.432′	100° 08.499′	13.555	6.348	27.456	3.895	14.516	2.178	7.968	27.198	0.351	2.554	0.600	1.686	0.215	2.798	0.765
147b	8.0	13° 06.399′	100° 09.585′	13.469	7.324	31.387	5.378	2.898	3.653	5.726	95.223	0.547	3.613	0.881	2.414	0.359	3.182	0.816
148a	9.0	13° 06.399′	100° 09.585′	13.174	3.767	21.425	3.484	12.446	2.537	6.287	68.213	0.477	2.359	0.689	1.575	0.194	1.997	0.527
148b	9.0	13° 06.399′	100° 09.585′	16.583	7.656	32.878	5.284	2.319	3.176	7.218	1.644	0.463	3.699	0.994	2.447	0.321	3.313	0.855
148c	5.0	13° 02.753′	100° 08.132′	2.556	8.519	34.982	5.659	2.678	2.813	8.660	132.667	0.547	4.246	1.755	2.731	0.314	3.639	0.928
149a	5.0	13° 02.753′	100° 08.132′	18.524	6.135	28.644	4.763	15.135	2.656	6.699	15.846	0.561	3.825	0.887	1.913	0.268	3.683	0.869
149c	15.0	13° 02.779′	100° 07.041′	5.384	2.993	12.777	1.778	6.521	0.815	3.640	9.736	0.197	0.783	0.174	0.545	0.443	0.960	0.285
150a	16.0	13° 02.779′	100° 07.041′	28.364	12.797	49.756	8.153	31.713	5.764	14.352	255.957	0.970	7.117	1.849	4.578	0.717	6.172	1.768
150c	11.0	13° 01.046′	100° 06.946′	3.953	15.749	56.144	8.948	34.840	6.148	15.299	235.495	1.181	7.898	1.735	4.575	0.689	6.433	1.685
151a	17.0	13° 01.046′	100° 06.946′	12.767	7.140	32.573	5.420	19.507	3.497	4.619	8.199	0.527	3.474	0.894	2.449	0.442	4.724	1.116
151c	18.0	13° 00.511′	100° 04.526′	15.661	9.400	36.513	5.238	19.387	3.853	8.338	44.677	0.492	3.371	0.763	2.283	0.315	3.247	0.843
152c	16.0	13° 00.511′	100° 04.526′	1.231	2.218	14.911	2.689	8.690	0.513	3.248	53.752	0.135	1.627	0.433	1.154	0.662	1.471	0.382
153a	7.5	13° 02.709′	100° 06.069′	15.547	5.524	26.428	4.376	17.448	3.218	6.734	12.451	0.529	3.683	0.877	2.386	0.352	3.322	0.839

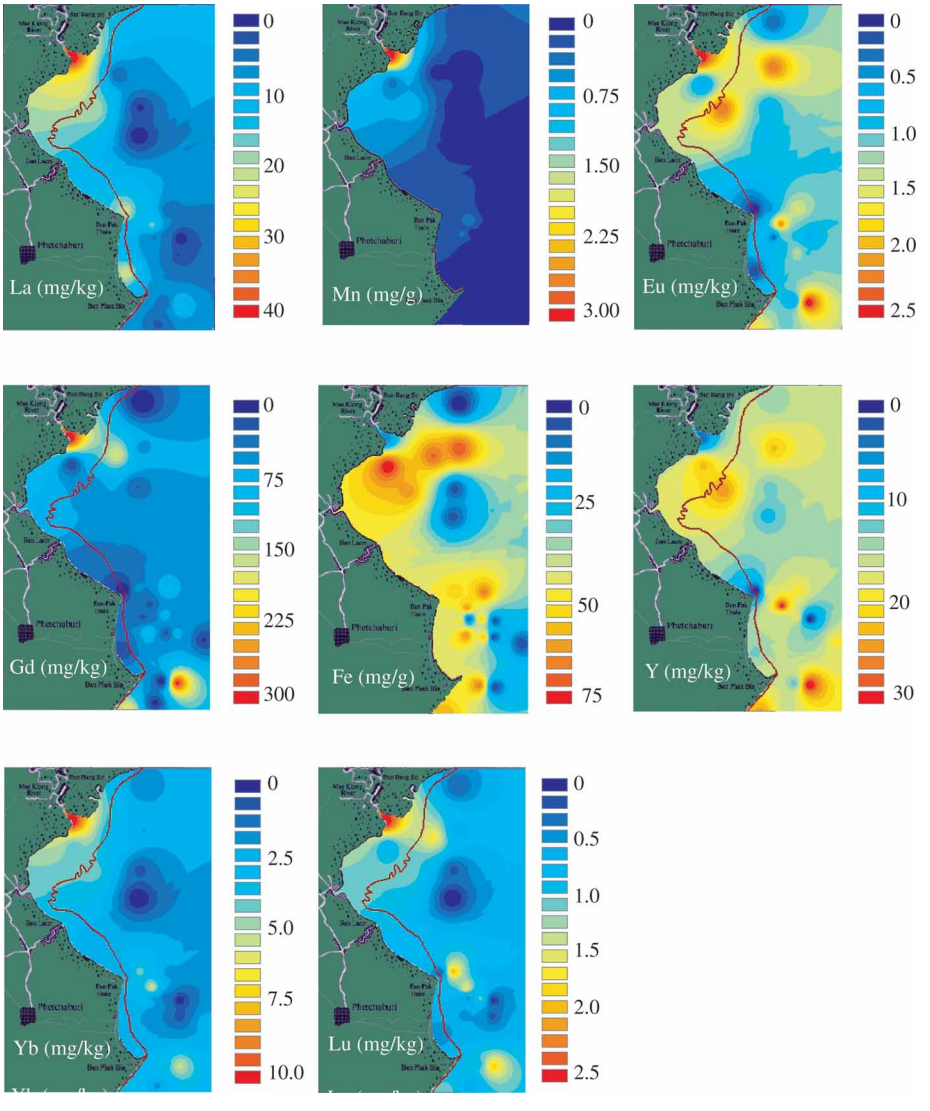

Figure 3. Schematic distributions of selected rare earth elements and Y from suspended matter in surface water samples. For further details on the statistical treatment of chemical data, see text. Red lines indicate the seaward limit of the tidal flat.

4. Discussion

4.1 *Dissolved phases*

The large similarities occurring in the area distributions of LREE and Y in dissolved samples coming from the surface waters seem to be influenced by riverine inputs and current regimes reported in the studied area [28]. Only eastern stations show REY concentration values similar to those reported for coastal waters [34] and coastal marine environments [13]. Conversely, the HREE concentrations (see the example of Yb and Lu in figure 2) show a maximum in the north-eastern study area.

Table 4. Station numbers and REE concentrations (mg kg^{-1}) in seafloor sediments from the studied sampling sites.

Station	Latitude (North)	Longitude (East)	La mg kg^{-1}	Ce mg kg^{-1}	Pr mg kg^{-1}	Nd mg kg^{-1}	Sm mg kg^{-1}	Eu mg kg^{-1}	Gd mg kg^{-1}	Tb mg kg^{-1}	Dy mg kg^{-1}	Ho mg kg^{-1}	Er mg kg^{-1}	Tm mg kg^{-1}	Yb mg kg^{-1}	Lu mg kg^{-1}
TH128	13° 15.883′	100° 04.457′	30.048	53.539	5.482	22.345	4.505	0.850	3.407	0.556	2.986	0.564	1.553	0.232	1.335	0.200
TH129	13° 17.931′	100° 05.451′	34.180	38.896	3.597	15.772	3.383	0.636	2.851	0.500	2.881	0.565	1.490	0.247	1.464	0.221
TH130	13° 20.450′	100° 04.212′	27.180	43.173	4.290	18.147	3.672	0.678	3.024	0.519	2.891	0.560	1.529	0.246	1.443	0.215
TH131	13° 21.228′	100° 06.419′	21.283	44.259	4.567	19.712	4.092	0.797	3.257	0.533	2.904	0.566	1.295	0.224	1.261	0.168
TH132	13° 24.100′	100° 06.400′	36.374	69.293	7.184	30.394	5.987	0.938	4.617	0.764	4.022	0.789	2.244	0.333	1.963	0.297
TH133	13° 18.555′	100° 01.997′	11.567	19.867	1.971	8.584	1.738	0.356	1.417	0.244	1.334	0.260	0.704	0.109	0.632	0.096
TH134	13° 17.906′	100° 00.850′	21.988	42.996	4.366	18.897	3.874	0.691	3.199	0.542	2.958	0.599	1.621	0.251	1.489	0.218
TH136	13° 05.493′	100° 04.428′	20.992	28.605	2.721	12.056	2.517	0.428	2.064	0.371	1.969	0.395	1.034	0.169	1.006	0.148
TH138	13° 10.166′	100° 05.036′	10.095	14.103	1.237	6.484	1.453	0.224	1.234	0.204	1.130	0.219	0.473	0.102	0.547	0.096
TH139	13° 10.359′	100° 05.745′	11.625	22.494	2.212	10.129	2.094	0.373	1.756	0.298	1.654	0.331	0.832	0.139	0.839	0.123
TH140	13° 10.250′	100° 07.945′	16.945	35.134	3.577	15.865	3.312	0.666	2.780	0.456	2.519	0.506	1.421	0.218	1.329	0.203
TH141	13° 07.945′	100° 08.229′	15.211	32.514	3.330	14.474	3.102	0.595	2.432	0.394	2.109	0.402	1.005	0.161	0.931	0.146
TH142	13° 08.141′	100° 07.332′	17.455	28.104	2.710	12.099	2.585	0.502	2.250	0.398	2.280	0.457	1.223	0.205	1.163	0.176
TH143	13° 08.068′	100° 06.537′	20.064	29.564	2.820	12.549	2.631	0.509	2.238	0.381	2.163	0.449	1.263	0.203	1.256	0.196
TH144	13° 07.883′	100° 05.989′	9.629	23.487	2.396	10.704	2.332	0.429	2.005	0.325	1.741	0.378	0.881	0.141	0.843	0.123
TH145	13° 08.905′	100° 06.102′	18.700	31.528	3.091	13.747	2.923	0.560	2.547	0.474	2.496	0.540	1.366	0.254	1.278	0.231
TH146	13° 06.586′	100° 06.303′	9.649	19.779	1.974	8.898	1.945	0.373	1.706	0.299	1.542	0.326	0.850	0.138	0.796	0.123
TH147	13° 06.480′	100° 07.861′	14.007	28.699	2.893	12.784	2.642	0.505	2.210	0.377	2.014	0.406	1.065	0.174	0.981	0.151
TH148	13° 06.432′	100° 08.499′	7.070	12.005	1.115	5.271	1.123	0.212	0.992	0.180	0.954	0.185	0.400	0.088	0.436	0.073
TH149	13° 06.399′	100° 09.585′	12.414	28.172	2.823	12.649	2.678	0.510	2.284	0.393	2.171	0.437	1.175	0.184	1.062	0.155
TH150	13° 02.753′	100° 08.132′	5.652	11.601	1.131	5.414	1.088	0.201	0.893	0.149	0.769	0.155	0.333	0.065	0.388	0.055
TH151	13° 02.779′	100° 07.041′	13.563	22.351	2.128	9.721	2.028	0.320	1.727	0.289	1.595	0.317	0.821	0.139	0.837	0.125
TH152	13° 01.046′	100° 06.946′	12.393	29.866	3.003	13.359	2.820	0.520	2.368	0.393	2.112	0.417	1.103	0.171	1.007	0.137
TH153	13° 00.511′	100° 04.526′	4.489	6.782	0.584	3.087	0.668	0.017	0.417	0.070	0.276	0.039	0.069	0.016	0.051	0.011

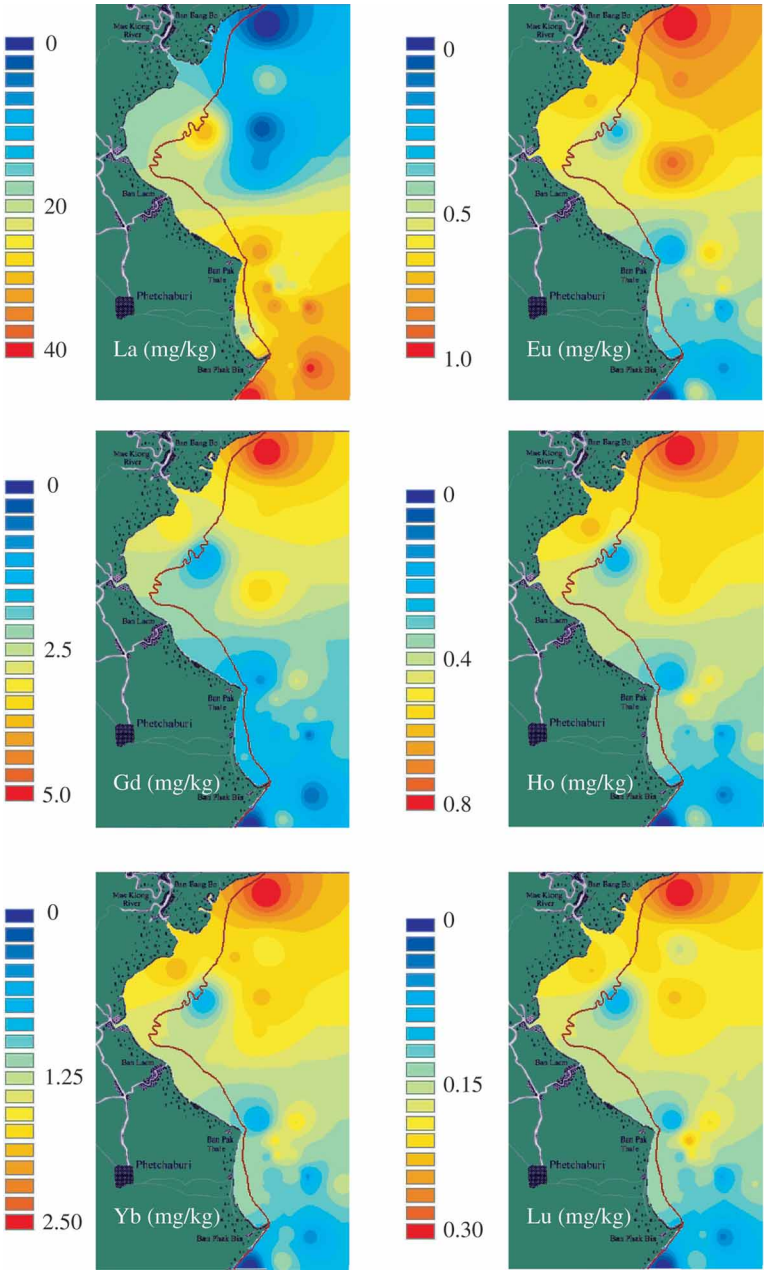

Figure 4. Schematic distributions of selected rare earth elements from seafloor sediments. For further details on the treatment of chemical data, see text. Red lines indicate the seaward limit of the tidal flat.

The input of large amounts of REE by rivers in the study area can be explained by a high-weathering effect on the REE sedimentary deposits occurring in the close continental region [35]. These introduce an important component of dissolved REE that in the river systems exists both as 'truly dissolved' organic complexes and in an organic-mediated colloidal form (0.025–0.22 μm). The colloidal pool produced by the river flow exhibits coagulation due to the increase in salt contents in the mixing zone among waters with different salinity values

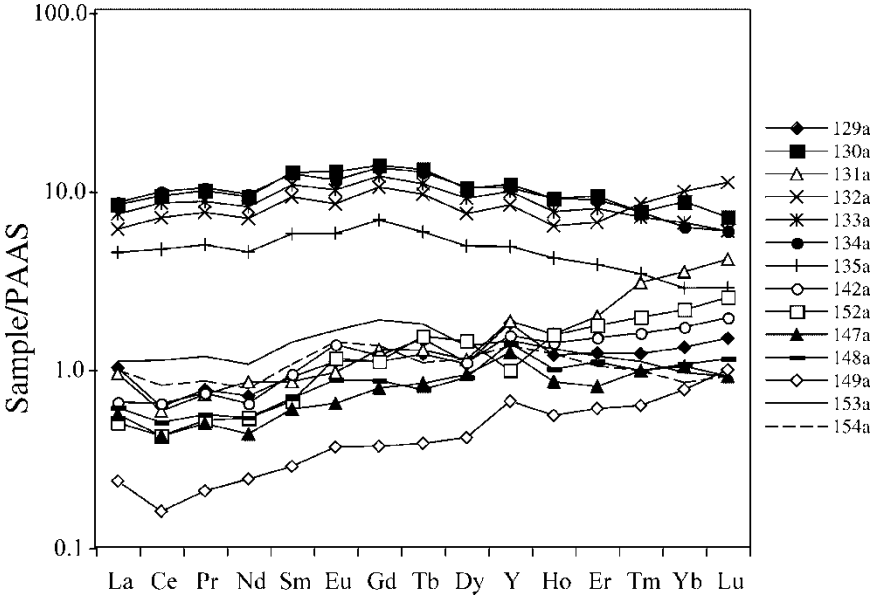

Figure 5. Shale-normalized REY patterns [29] in the dissolved phase of selected water samples.

under estuarine environmental conditions, transferring the REE charge from the colloidal phase to an authigenic particulate fraction. This scavenging process is responsible for the lower concentration values of REY measured in the estuarine area of the Mae Klong river. Moreover, the coagulation of colloidal pool could explain the preferential removal of LREE over HREE in the low-salinity coastal areas [36] close to the Mae Klong mouth and may explain the different behaviours observed among LREE and HREE and described in figure 2. Under these conditions, Y and La show very similar behaviour, according to the higher covalent contribution to the bonding of Y and La during the complexation effect with solution ligands with respect to HREE [1]. Moreover, the shale-normalized REY behaviour shows an increasing REE content, the disappearance of the Ce negative anomaly typical of seawaters, and the

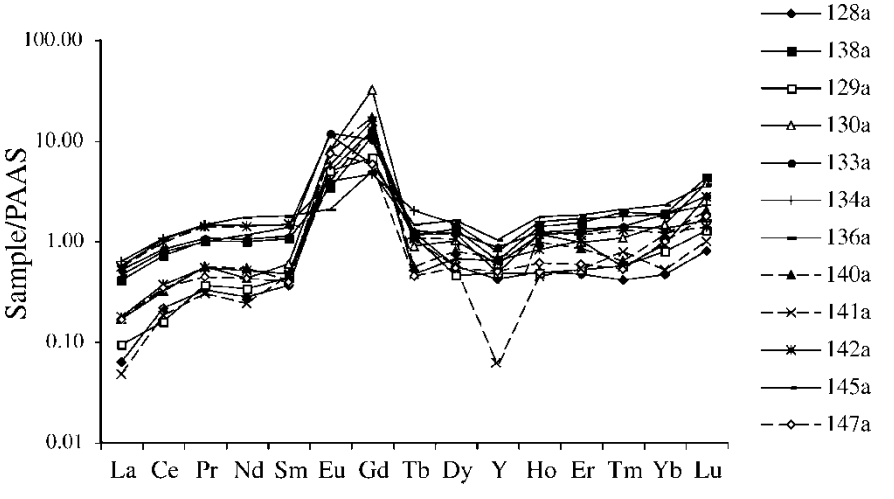

Figure 6. Shale-normalized REY patterns [29] in suspended matter from selected water samples.

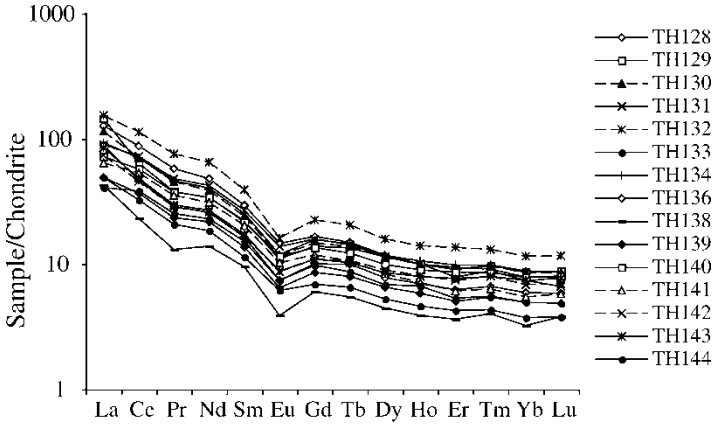

Figure 7. Chondrite-normalized REE patterns [33] of selected seafloor sediments.

occurrence of a positive Ce anomaly related to a preferential enrichment of Ce onto colloidal particles relative to La and Nd. This evidences suggest that river colloids can provide surface sites for Ce accumulation as a consequence of Ce^{3+} oxidation to Ce^{4+} [36]. This phenomenon could explain the similarities among the shale-normalized REE patterns of 'dissolved' phases in our samples and the shale-normalized REE patterns of the labile fraction of suspended particulate matter. Therefore, we assume that the filtration of water samples, carried out using a 0.2 μm membrane, was not able to select colloidal pool from the dissolved one, and the study samples contain REE both in the colloidal phase and in the dissolved pool. Consequently, the behaviours of shale-normalized REY patterns are as follows:

- Typical seawater behaviour occurs only in samples from the eastern zone with a higher salinity content and where Ce negative anomalies and HREE/LREE fractionation are evident.
- There is a pronounced convexity centred on the intermediate REE, Eu, and Gd, due to depletions of LREE relative to Eu and Gd. If this depletion is greater than that between Gd and Lu, the resulting patterns are similar to those reported for some intermediate and bottom waters. This behaviour is in agreement with the occurrence of a large colloidal pool in water samples. The presence of both a dissolved and a colloidal fraction in samples, in different relative amounts, justifies the observed 'convexity' caused by the simultaneous occurrence of an HREE enrichment typical of the dissolved fraction and an LREE enrichment typical of colloidal pool when REY concentrations are normalized to shale [37].
- There is a flat behaviour probably induced by the large REE contents in the colloidal pool which, with its shale-like pattern compared with the HREE enriched pattern of the dissolved pool alone, contributes a greater proportion of LREE than HREE to the total REE content of waters.
- There are Gd anomalies ranging from 1.05 to 1.3.

4.2 *Particulate matter*

As discussed above, when river water reaches the estuarine/seawater mixing zone, the removal of REY induced by salt coagulation of the river colloidal pool takes place, producing the authigenic fraction of suspended particulate matter. This removal leads to REE fractionation because LREE are more easily scavenged than HREE [38]. The differences observed among the behaviour of Y and other REE are not a radius-controlled effect but probably induced

by differences in the 4f electronic configuration of Y and REE that are reflected in different surface complexation behaviours [8, 34, 39].

In order to distinguish between the mechanisms and the processes controlling the REY removal in the mixing zone and to recognize the different fractions of suspended particulate matter, we tested whether there was any relationship between Fe and Mn contents [24] and REE distributions in particulate matter because both Fe and Mn have a very distinctive behaviour in the estuarine mixing interface environment.

According to this evidence, a strong Fe–REE relationship in suspended particulate matter indicates that large-scale removal of these elements from the dissolved pool to suspended particulate matter took place in terms of coagulation of Fe by sea salt, normally organically stabilized in colloidal form in low-saline river waters [13].

In contrast, if REE contents in suspended particulate matter are related to Mn contents, redox processes are responsible for simultaneous REE and Mn scavenging from dissolved to particulate phases because Mn occurs primarily as inorganic complexes [40], and its removal onto suspended particles takes place by oxidation and scavenging. The occurrence of this process has been reported in suspended particulate matter from bottom waters of external stations, in the eastern and southern parts of the studied area.

Correlation matrices of Mn–Fe–REY distribution data calculated for the suspended particulate matter confirm a very similar behaviour of Mn and all REE, thus allowing us to presume that there is an oxidative scavenging process in shallow, less saline waters. Moreover, the weak correlations among Fe and REY reported in suspended particulate from intermediate water layers (table 5) indicate that REY behaviours cannot be explained simply in terms of salt-induced coagulation of the colloidal pool.

The weak correlations among Eu, Gd, and other trace elements are determined by their different origins or behaviour during processes that led to the formation of the authigenic particulate matter.

The coagulation of organically stabilized Fe-colloids occurring in river waters and induced by sea salts under estuarine conditions:

- provides a large Fe release in the mangrove coastal environment; and
- transfers the REY contents of the colloids to the suspended authigenic fraction as a consequence of the release of REY to the truly dissolved fraction.

We presume that the environmental conditions occurring in the studied mangrove coastal area, with a low pH [41], cause both the Eu and Gd observed anomalies. The phenomenon could be a two-step process:

1. Eu is removed from the dissolved phase and scavenged to preferentially occupy Ca^{2+} sites in the newly formed authigenic fraction of both carbonate [42] and clay minerals, which operate as an 'Eu pumping system' whose ability to retain Eu is greater at pH values close to 5.5 [43], as in the studied environment [28].
2. Gd and other medium REE (MREE) enrichments observed in particulate matter are induced by coagulation of colloidal materials coming from river waters during the formation of the authigenic particulate fraction. These enrichments were previously reported in other rivers from the Papua New Guinea area and explained as a result of preferential release of Gd and MREE in the dissolved pool of river waters defined as an 'island weathering signature' [44].

To distinguish between the occurrences of authigenic and lithogenic fractions in suspended particulate matter, a useful approach uses Y/Ho ratios and Eu/Eu^* values. If a geochemical

Table 5. Correlation matrices calculated for REY concentrations measured in suspended particulates of surface, intermediate, and bottom waters.

	Mn	Fe	Y	La	Ce	Pr	Nd	Sm	Eu	Gd	Tb	Dy	Ho	Er	Tm	Yb	Lu
Surface waters																	
Mn	1.00																
Fe	0.13	1.00															
Y	−0.10	0.47	1.00														
La	0.64	0.29	0.18	1.00													
Ce	0.62	0.25	0.14	0.92	1.00												
Pr	0.65	0.21	0.00	0.88	0.92	1.00											
Nd	0.65	0.17	0.15	0.82	0.87	0.82	1.00										
Sm	0.64	0.30	0.17	0.92	0.96	0.91	0.84	1.00									
Eu	0.05	0.11	0.49	0.21	0.11	0.04	0.18	0.14	1.00								
Gd	0.22	−0.22	0.08	0.19	0.13	0.25	0.23	0.20	0.65	1.00							
Tb	0.59	0.23	0.13	0.83	0.86	0.80	0.80	0.85	0.22	0.33	1.00						
Dy	0.71	0.06	0.09	0.65	0.66	0.63	0.66	0.73	0.34	0.51	0.68	1.00					
Ho	0.64	0.18	0.21	0.84	0.84	0.81	0.85	0.88	0.45	0.55	0.85	0.85	1.00				
Er	0.64	0.30	0.33	0.88	0.90	0.83	0.88	0.92	0.36	0.40	0.89	0.79	0.96	1.00			
Tm	0.58	0.15	0.17	0.74	0.73	0.70	0.75	0.79	0.25	0.32	0.74	0.68	0.80	0.82	1.00		
Yb	0.10	0.53	0.79	0.45	0.45	0.31	0.40	0.50	0.21	−0.04	0.39	0.26	0.41	0.53	0.42	1.00	
Lu	0.42	0.28	0.37	0.58	0.52	0.49	0.56	0.60	0.59	0.63	0.58	0.73	0.83	0.79	0.66	0.49	1.00
Intermediate waters																	
Mn	1.00																
Fe	0.13	1.00															
Y	−0.10	0.47	1.00														
La	0.64	0.29	0.18	1.00													
Ce	0.62	0.25	0.14	0.92	1.00												
Pr	0.65	0.21	0.00	0.88	0.92	1.00											
Nd	0.65	0.17	0.15	0.82	0.87	0.82	1.00										
Sm	0.64	0.30	0.17	0.92	0.96	0.91	0.84	1.00									
Eu	0.05	0.11	0.49	0.21	0.11	0.04	0.18	0.14	1.00								
Gd	0.22	−0.22	0.08	0.19	0.13	0.25	0.23	0.20	0.65	1.00							
Tb	0.59	0.23	0.13	0.83	0.86	0.80	0.80	0.85	0.22	0.33	1.00						
Dy	0.71	0.06	0.09	0.65	0.66	0.63	0.66	0.73	0.34	0.51	0.68	1.00					
Ho	0.64	0.18	0.21	0.84	0.84	0.81	0.85	0.88	0.45	0.55	0.85	0.85	1.00				
Er	0.64	0.30	0.33	0.88	0.90	0.83	0.88	0.92	0.36	0.40	0.89	0.79	0.96	1.00			
Tm	0.58	0.15	0.17	0.74	0.73	0.70	0.75	0.79	0.25	0.32	0.74	0.68	0.80	0.82	1.00		
Yb	0.10	0.53	0.79	0.45	0.45	0.31	0.40	0.50	0.21	−0.04	0.39	0.26	0.41	0.53	0.42	1.00	
Lu	0.42	0.28	0.37	0.58	0.52	0.49	0.56	0.60	0.59	0.63	0.58	0.73	0.83	0.79	0.66	0.49	1.00
Bottom waters																	
Mn	1.00																
Fe	−0.03	1.00															
Y	0.30	−0.10	1.00														
La	0.48	0.37	0.24	1.00													
Ce	0.56	0.18	0.66	0.70	1.00												
Pr	0.60	0.22	0.64	0.70	0.99	1.00											
Nd	0.52	0.12	0.76	0.60	0.87	0.87	1.00										
Sm	0.55	0.17	0.64	0.80	0.96	0.95	0.89	1.00									
Eu	0.09	0.10	−0.12	0.65	0.36	0.35	0.26	0.48	1.00								
Gd	0.10	0.31	0.09	0.55	0.44	0.46	0.35	0.50	0.73	1.00							
Tb	0.31	−0.08	0.51	0.53	0.55	0.56	0.63	0.71	0.51	0.58	1.00						
Dy	0.43	0.14	0.57	0.70	0.92	0.91	0.83	0.92	0.57	0.72	0.74	1.00					
Ho	0.37	−0.04	0.52	0.50	0.79	0.78	0.63	0.75	0.42	0.71	0.61	0.89	1.00				
Er	0.42	0.09	0.66	0.61	0.91	0.91	0.83	0.90	0.45	0.69	0.70	0.98	0.93	1.00			
Tm	0.04	−0.17	0.02	0.00	−0.15	−0.12	0.20	−0.01	0.10	0.22	0.54	0.12	−0.02	0.06	1.00		
Yb	0.38	0.19	0.55	0.72	0.91	0.91	0.81	0.92	0.58	0.73	0.76	0.99	0.87	0.96	0.11	1.00	
Lu	0.29	0.23	0.50	0.70	0.85	0.85	0.80	0.88	0.63	0.76	0.76	0.97	0.83	0.93	0.18	0.98	1.00

system is driven by CHARAC REY behaviour [3], trace elements with a similar charge and dimensions to Y^{3+} and Ho^{3+} or Eu^{2+}, Sr^{2+}, and Ca^{2+} should show a coherent behaviour, as in lithogenic conditions. In contrast, in aquatic systems, the complexation–adsorption behaviour of the trace elements does not depend exclusively on CHARAC characters, and their electronic configuration plays a fundamental role in decoupling the Y and Ho behaviour due to the difference in the covalent character of bonding between Y^{3+} and Ho^{3+} because Y^{3+} uses 4d orbitals to create chemical bonds, whereas Ho^{3+} has 4f orbitals available.

For example, under lithogenic conditions, Eu is easily stable as Eu^{2+} and, in eightfold coordinations, has an ionic radius similar to Ca^{2+}; in the marine environment, it is essentially stable as Eu^{3+}, and in this ionic configuration, it has undergone CHARAC coprecipitation with authigenic calcite, its ionic radius (0.95 Å) being similar to that of Ca^{2+} (1.00 Å) [44–45]. However, the similarities occurring in Eu and Fe distributions (figure 3) indicate that scavenging of dissolved Eu onto surfaces of suspended particulate matter is a non-CHARAC process but it is induced by increase of salt contents of waters that drives the coagulation of Fe-rich colloids. It takes place to an active surface to adsorb the dissolved Eu^{3+} according to a process that is sensitive to the ionic strength [43].

According to the above-mentioned ideas, samples containing large autigenic particulate fractions are expected to show low Y/Ho ratios and Eu/Eu* values higher than those reported in seafloor sediments. On the contrary, a greater lithogenic contribution to the suspended particulate matter should be represented by higher Y/Ho ratios and lower Eu/Eu* values. Finally, Y/Ho values in the dissolved phase should fall within the range of seawater values with an Eu/Eu* signature similar to the composition of seafloor sediments. The studied samples of suspend particulate samples fall in the area characteristic of Fe–Mn oxydroxides crusts and only in a few cases into the 'lithogenic' range of CHARAC values (figure 8), in agreement with CHARAC co-precipitation of Eu in authigenic calcite. Moreover, the dissolved phase of the study samples shows an excellent agreement with the 'normal' marine composition (figure 8).

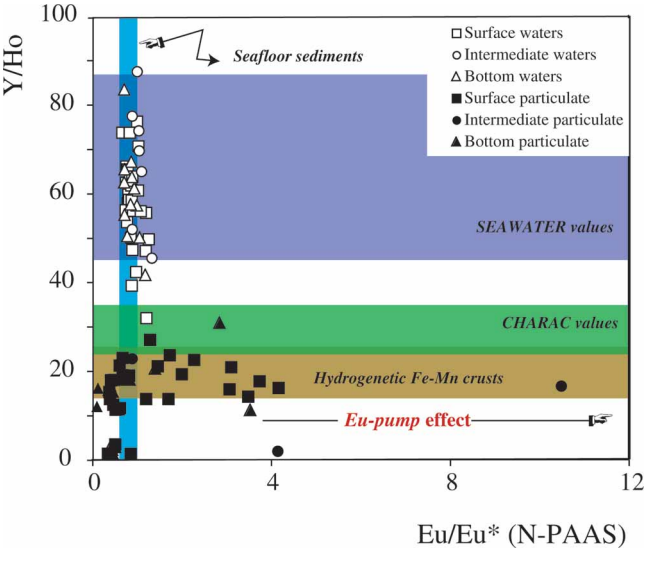

Figure 8. Y/Ho and Eu/Eu* values in suspended particulate and dissolved phase of the studied samples. Typical seawater field, CHARAC, and hydrogenic Fe–Mn crusts fields are depicted according to the literature [3].

4.3 *Sediments*

The chondrite-normalized REY patterns reported for the sediments collected in the studied area show geochemical features typical of continental rocks that underwent extensive weathering processes occurring without fractionation among the different REE. Moreover, they appear very similar to those reported for various Malaysian peninsular batholiths [20, 46].

5. Conclusions

In the coastal waters of the Western Part of the Gulf of Thailand, the so-called 'Inner Gulf', high concentrations of REE occur both in the dissolved phase and in particulate suspended matter. The origin of these anomalous concentrations and distributions appears strictly related to extensive rock–water interaction processes occurring in the hydrologic basin of the Mae Klong and Phetchaburi rivers. Here, widespread alterations of REE-rich materials, probably phosphates of secondary origin, occur and justify the large input of REE in dissolved and suspended phase in the coastal marine area. During rock–water interactions in the continental environment, weathered REE were distributed in dissolved and colloidal pools, while a detrital, weathered fraction was carried out in the river flow to form the seafloor coastal sediments. The extent of fractionation and then the distribution of REE in the river water systems were determined by the competition among particle surfaces, colloidal surfaces, and solution ligands. When the entire 'dissolved' REE load arrives in the estuarine interface environment, coagulation of colloidal pool and a large-scale removal of REE from dissolved and colloidal pools takes place, transferring to the particulate authigenic fraction part of the REE from the 'dissolved' phases, while the REY concentration of sediments explains the more weathered and residual rock fraction.

Acknowledgements

This work was supported by a grant (COFIN 2001) from Italian MIUR.

References

[1] M. Bau. Scavenging of dissolved yttrium and rare earths by precipitation iron oxydroxide: Experimental evidence for Ce oxidation, Y/Ho fractionation, and lanthanide tetrad effect. *Geochim. Cosmochim. Acta*, **63**, 67–77 (1999).
[2] G.A. McKay. Partitioning of Rare Earth Elements between major silicate minerals and basaltic melts. In B.R. Lipin, G.A. McKay (Eds.), *Geochemistry and Mineralogy of Rare Earth Elements. Reviews in Mineralogy Vol. 21*, pp. 45–75, Washington, D.C., (1989).
[3] M. Bau. Controls on the fractionation of isovalent trace elements in magmatic and aqueous systems: evidence from Y/Ho, Zr/Hf, and lanthanide tetrad effect. *Contrib. Miner. Petrol.*, **123**, 323 (1996).
[4] K.J. Cantrell, R.H. Byrne. Rare earth elements complexation by carbonate and oxalate ions. *Geochim. Cosmochim. Acta*, **51**, 597 (1987).
[5] S.A. Wood. The aqueous geochemistry of rare earth elements and yttrium, I. Review of available low-temperature data for inorganic complexes and the inorganic REE speciation of natural waters. *Chem. Geol.*, **82**, 159 (1990).
[6] F. Millero. Stability constants for the formation of rare earth inorganic complexes as a function of ionic strength. *Geochim. Cosmochim. Acta*, **56**, 3123 (1992).
[7] J.H. Lee, R.H. Byrne. Examination of comparative rare earth complexation behaviour using linear free-energy relationships. *Geochim. Cosmochim. Acta*, **56**, 1127 (1992).
[8] R.H. Byrne, J.H. Lee. Comparative yttrium and rare earth element chemistries in seawater. *Mar. Chem.*, **44**, 121 (1993).
[9] Y. Takahashi, Y. Minai, S. Ambe, Shizuko; Y. Makide, F. Ambe, Simultaneous determination of stability constants of humate complexes with various metal ions using multitracer technique. *Sci. Tot. Environ.*, **198**, 61 (1997).
[10] T. Wyndham, M. McCulloch, S. Fallon, C. Alibert. High-resolution coral records of rare earth elements in coastal seawater: biogeochemical cycling and a new environmental proxy. *Geochim. Cosmochim. Acta*, **68**, 2067 (2004).

[11] J.M. Martin, O. Hogdahl, J.C. Phillipot. Rare earth element supply to the oceans. *J. Geophys. Res.*, **81**, 3119 (1976).
[12] S.J. Goldstein, S.B. Jacobsen. Rare earth elements in river waters. *Earth Planet. Sci. Lett.*, **89**, 35 (1988).
[13] H. Elderfield, R. Upstill-Goddard, E.R. Sholkovitz. The rare earth elements in rivers, estuaries and coastal sea waters: Processes affecting crustal input of elements to the ocean and their significance to the composition of sea water. *Geochim. Cosmochim. Acta*, **54**, 971 (1990).
[14] E.R. Sholkovitz. Chemical evolution of rare earth elements: Fractionation between colloidal and solution phases of filtered river water. *Earth Planet. Sci. Lett.*, **114**, 77 (1992).
[15] J. Hoyle, H. Elderfield, A. Gledhill, M. Greaves. The behaviour of rare earth elements during mixing of river and sea waters. *Geochim. Cosmochim. Acta*, **48**, 143 (1984).
[16] P. Möller, M. Bau. Rare-earth patterns with positive cerium anomaly in alkaline lake waters from lake Van, Turkey. *Earth Planet. Sci. Lett.*, **117**, 671 (1993).
[17] K.H. Johannesson, W.B. Lyon. The rare earth element geochemistry of Mono Lake water and the importance of carbonate complexing. *Limnol. Oceanogr.*, **39**, 1141 (1994).
[18] K.H. Johannesson, W.B. Lyon. Rare-earth element geochemistry of Color lake, an acidic freshwater lake on Axel Heiberg Island, Northwestern Territories, Canada. *Chem. Geol.*, **119**, 209 (1995).
[19] K.H. Johannesson, W.B. Lyon, M.A. Yelken, H.E. Gaudette, K.J. Statzebach. Geochemistry of rare-earth elements in hypersaline and diluite acidic natural terrestrial waters: Complexation behaviour and middle rare-earth element enrichments. *Chem. Geol.*, **133**, 125 (1996).
[20] M.O. Schwartz, S.S. Rajan, A.K. Askury, P. Putthapiban, S. Djaswadi. The Southern Asian Tin Belt. *Earth Sci. Rev.*, **38**, 95–293 (1995).
[21] K. Srisuksawad, B. Pornterkasemsan, N. Sunun, Y. Pathom, R. Carpenter, M.L. Peterson, T. Hamilton. Radionuclide activities, geochemistry, and accumulation rates of sediments in the Gulf of Thailand. *Continent. Shelf Res.*, **17**, 925–965 (1997).
[22] S. Tanabe, Y. Saito, Y. Sato, Y. Suzuki, S. Sinsakul, S. Tiypairach, N. Chaimanee. Stratigraphy and Holocene evolution of the mud-dominated Chao Phraya delta, Thailand. *Quatern. Sci. Rev.*, **22**, 789–807 (2003).
[23] L. Oyebande, J. Balek. Humid warm sloping land. In *Comparative Hydrology. An Ecological Approach to Land and Water Resources*, M. Falkenmark, T. Chapman (Eds.), pp. 224–274, UNESCO, Paris (1988).
[24] P. Censi, S.E. Spoto, G. Nardone, M. Sprovieri, F. Saiano, D. Ottonello, S.E. Di Geronimo. Heavy metal contents in coastal water systems. A case of study in the North-western Gulf of Thailand. *Chemosphere* (accepted).
[25] A.J. Paulson. The effects of flow rate and pre-treatment on the analyses of trace metals in estuarine and coastal seawater by Chelex-100. *Anal. Chem.*, **58**, 183 (1986).
[26] P. Möller, P. Dulski, J. Luck. Determination of rare earth elements in seawater by inductively coupled plasma-mass spectrometry. *Spectrochim. Acta*, **47B**, 1379 (1992).
[27] C. Barbante, G. Cozzi, G. Capodaglio, K. Van de Velde, C. Ferrari, C. Boutron, P. Cescon. Trace element determination in alpine snow and ice by double focusing inductively coupled plasma mass spectrometry with microcentric nebulization. *J. Anal. Atom. Spectrosc.*, **14**, 1433 (1999).
[28] N. Chaimanee, I. Di Geronimo, E. Robba, R. Sanfilippo. Modern environments and Holocene evolution on the west coast of the upper gulf of Thailand, paper presented at *Proceedings of Congress 'The Comprehensive Assessments on Impacts of Sea-Level Rise'*, Petchaburi, Thailand, pp. 35–59 (1999).
[29] S.R. Taylor, S.M. McLennan. *The Continental Crust: Its Composition and Evolution.* Blackwell Scientific, Oxford (1985).
[30] E.R. Sholkovitz. Rare earth elements in the sediments of the North Atlantic Ocean, Amazon delta, and East China Sea: Reinterpretation of terrigenous input patterns to the oceans. *Am. J. Sci.*, **288**, 236 (1988).
[31] Y. Nozaki, J. Zhang, H. Amakawa. The fractionation between Y and Ho in the marine environment. *Earth Planet. Sci. Lett.*, **148**, 329 (1997).
[32] S.S. Sun. W.F. McDonough. Chemical and isotopicsystematics of oceanic basalts. In D. Saunders & M.J. Norry (Eds.), *Magmatism in the Ocean Basins. Geol. Soc. Am. Bull.*, **42**, 313 (1989).
[33] D.S. Alibo, Y. Nozaki. Rare earth elements in seawater: Particle association, shale-normalization, and Ce oxidation. *Geochim. Cosmochim. Acta*, **63**, 363 (1999).
[34] Y. Nozaki, D. Lerche, D.S. Alibo, A. Snidvongs. The estuarine geochemistry of rare earth elements and indium in the Chao Phraya River, Thailand. *Geochim. Cosmochim. Acta*, **64**, 3983 (2000).
[35] G.J. Orris, R.I. Grauch. *Rare Earth Elements Mines, Deposits, and Occurrences.* USGS Open File Report 02-189 (2002).
[36] E.R. Sholkovitz. Chemical evolution of rare earth elements: fractionation between colloidal and solution phases of filtered river water. *Earth Planet. Sci. Lett.*, **114**, 77 (1992).
[37] K.K. Bertine, R. VernonClark. Elemental composition of the colloidal phase isolated by cross-flow filtration from coastal seawater samples. *Mar. Chem.*, **55**, 189 (1996).
[38] E.R. Sholkovitz. The geochemistry of rare earth elements in the Amazon River estuary. *Geochim. Cosmochim. Acta*, **57**, 2181 (1993).
[39] K.A. Quinn, R.H. Byrne, J. Schijf. Comparative scavenging of yttrium and the rare earth elements in seawater: Competitive influences of solution and surface chemistry. *Aquat. Geochem.*, **10**, 59 (2004).
[40] W. Stumm, J.J. Morgan. Aquatic chemistry, 2nd Edition. Wiley (1997)
[41] K. Boonsong, S. Piyatiratitivorakul, P. Patanapopaiboon. Effects of wastewater discharge on mangrove soils, paper presented at *Proceedings of 17th WCSS Congress*, 14–17 August 2002, 1901-1–1901-10 (2002).

[42] L.Z. Lakshtanov, S.L.S. Stipp. Experimental study of europium (III) co precipitation with calcite. *Geochim. Cosmochim. Acta*, **68**, 819 (2004).
[43] S.B. Clark, A.L. Bryce, A.D. Lueking, J. Gariboldi, S.M. Serkiz. Factor affecting trivalent f-elements to an acidic sandy soil. In Everette A.J. (Ed.), *Adsorption of Metals by Geomedia*, pp. 150–164, Academic Press, San Diego, CA (1998).
[44] E.R. Sholkovitz, H. Elderfield, R. Smymczak, K. Casey. Island weathering: river sources of rare earth elements to the Western Pacific Ocean. *Mar. Chem.*, **68**, 39 (1999).
[45] S.L.S. Stipp, L.Z. Lakshtanov, J.T. Jensen, J.A. Baker. Eu^{3+} uptake by calcite: preliminary results from co precipitation experiments and observations with surface sensitive techniques. *J. Contam. Hydrol.*, **61**, 33 (2003).
[46] T.C. Liew. Petrogenesis of the Peninsular Malaysian Granitoid Batholiths. PhD thesis, Canberra, Australian National University (1983).